CORE
Metadata, citation and similar papers at core.ac.uk
Provided by Elsevier - Publisher Connector

FEBS 29456 FEBS Letters 579 (2005) 2327–2333

Human mitochondrial peroxiredoxin 5 protects from mitochondrial DNA damages induced by hydrogen peroxide

Ingrid Banmeyer, Cécile Marchand, André Clippe, Bernard Knoops*

Laboratory of Cell Biology, Institut des Sciences de la Vie, Université catholique de Louvain, B-1348 Louvain-La-Neuve, Belgium

Received 14 January 2005; revised 10 March 2005; accepted 10 March 2005

Available online 24 March 2005

Edited by Barry Halliwell

Abstract Peroxiredoxin 5 is a thioredoxin peroxidase ubiquitously expressed in mammalian tissues. Peroxiredoxin 5 can be addressed intracellularly to mitochondria, peroxisomes, the cytosol and the nucleus. Here, we show that mitochondrial human peroxiredoxin 5 protects mitochondrial DNA (mtDNA) from oxidative attacks. In an acellular assay, recombinant peroxiredoxin 5 was shown to protect plasmid DNA from damages induced by metal-catalyzed generation of reactive oxygen species. In Chinese hamster ovary cells, overexpression of mitochondrial peroxiredoxin 5 significantly decreased mtDNA damages caused by exogenously added hydrogen peroxide. Altogether our results suggest that mitochondrial peroxiredoxin 5 may play an important role in mitochondrial genome stability.
© 2005 Federation of European Biochemical Societies. Published by Elsevier B.V. All rights reserved.

Keywords: Peroxiredoxin; Thioredoxin peroxidase; Antioxidant enzyme; Mitochondria; Peroxide

1. Introduction

Because of its close proximity to the electron transport chain, mitochondrial DNA (mtDNA) is highly exposed to oxidative attacks caused by reactive oxygen species (ROS) produced by electron leakage during oxidative phosphorylation [1]. Moreover, mtDNA is thought to be more susceptible to oxidative damages than nuclear DNA (nDNA) due to the lack of histones [2,3] and the vulnerability or the insufficiency of mitochondrial repair pathways [4,5]. Importantly, oxidative damage to mtDNA is now emerging as an etiological factor in oxidative stress-related disorders such as cardiovascular diseases, neurodegenerative diseases but also normal aging [6].

In addition to well documented antioxidant enzymes such as superoxide dismutases, catalase and gluthatione peroxidases, a family of peroxidases named peroxiredoxins (PRDXs) has been discovered more than a decade ago (for review see [7]). PRDXs are a superfamily of selenium-free and heme-free peroxidases able to catalyze the reduction of hydrogen peroxide, alkyl hydroperoxides and peroxynitrite [8–10]. In mammals, six PRDX isoforms (PRDX1–6) encoded by six different genes have been identified and characterized. PRDX3 and PRDX5 are the two mammalian PRDXs that are addressed to mitochondria [11,12]. Moreover, PRDX5 can be also addressed to peroxisomes, the cytosol and, to a lesser extent, to the nucleus [13].

Recently, we showed that overexpression of human PRDX5 in the nucleus of Chinese hamster ovary (CHO) cells decreases nDNA damages induced by exogenously applied peroxides [13]. Furthermore, peroxiredoxin-null yeast cells have been reported to display an increased rate of spontaneous nDNA mutations [14] and TSA1, a *Saccharomyces cerevisiae* peroxiredoxin, was found to play a significant role in suppression of nDNA mutations [15]. Moreover, it appears that in many mammalian cell types, PRDX5 is primarily addressed to mitochondria [11,16–18]. In view of this, the purpose of the current study was to further characterize the mitochondrial genoprotective function of mitochondrial PRDX5. First, using an acellular system composed of plasmid DNA, which resembles the structure of mtDNA, we investigated the protective effects of human recombinant PRDX5 against DNA damages induced by metal-catalyzed generation of ROS, the thiol/Fe^{3+}/O_2 mixed-function oxidase (MFO) system [19]. Second, the genoprotective properties of PRDX5 on mtDNA were examined in CHO cells overexpressing mitochondrial PRDX5 and exposed to exogenously added peroxides.

2. Materials and methods

2.1. Materials

Hydrogen peroxide (H_2O_2), *tert*-butylhydroperoxide (*t*BHP) and ethidium bromide were purchased from Sigma. The BCA protein assay reagent was from Pierce. Fetal bovine serum, Dulbecco's modified Eagle's media (DMEM), penicillin, streptomycin, L-glutamine and trypsin-EDTA were purchased from Life Technologies, Inc. All primers were obtained from Invitrogen. $FeCl_3$ was from Aldrich, DL-dithiothreitol (DTT) from Acros and Chelex-100 resin from Bio-Rad.

2.2. Expression and purification of recombinant proteins

Human PRDX5 [11] (GenBank Accession No. NM_012094), the short form without its mitochondrial pre-sequence, was expressed in *Escherichia coli* strain M15 (pRep4) as 6 × His-tagged protein using

*Corresponding author. Fax: +32 10 47 35 15.
E-mail address: knoops@bani.ucl.ac.be (B. Knoops).

Abbreviations: C47S-PRDX5, recombinant C47S mutant of human PRDX5; CCC, supercoiled plasmid DNA; CHO cells, Chinese hamster ovary cells; COX1, cytochrome C oxidase subunit 1; DTT, dithiothreitol; H_2O_2, hydrogen peroxide; MFO, thiol/Fe^{3+}/O_2 mixed-function oxidase; mtDNA, mitochondrial DNA; ND4, NADH dehydrogenase subunit 4 gene; nDNA, nuclear DNA; NLS, nuclear localization signal; nuc-PRDX5, nuclear human recombinant PRDX5; OC, open circular plasmid DNA; ·OH, hydroxyl radical; PRDX, peroxiredoxin; ROS, reactive oxygen species; *t*BHP, *tert*-butylhydroperoxide; wt-PRDX5, wild-type human recombinant PRDX5

0014-5793/$30.00 © 2005 Federation of European Biochemical Societies. Published by Elsevier B.V. All rights reserved.
doi:10.1016/j.febslet.2005.03.027

pQE-30 expression vector (Qiagen) and purified as described previously (wt-PRDX5) [20]. The mutated recombinant PRDX5 (C47S-PRDX5), in which the N-terminal catalytic Cys^{47} of the short form (amino acid numbering refers to mature protein) was replaced by a serine, was generated by standard PCR-mediated site-directed mutagenesis as reported in Plaisant et al. [21]. To produce a nuclear recombinant PRDX5 (nuc-PRDX5) [13] corresponding to the short form of PRDX5 in N-terminal fusion with the SV40 large-T antigen nuclear localization sequence, we amplified *nuc-PRDX5* DNA [13] by PCR using forward primer 5′-ACT AGT GGA TCC GGG CCA AAG AAG AAG CGA AAG-3′ (*Bam*HI site underlined) and reverse primer 5′-GTC GCA AGC TTG CCT CAG AGC TGT GAG ATG-3′ (*Hind*III site underlined). The PCR product was digested with *Bam*HI and *Hind*III, and ligated into the pQE-30 expression vector. The insert was sequenced and the additional N-terminal fusion with the 6 × His-tag was confirmed. The resulting vector was used to transform *E. coli* strain M15 (pRep4) and nuc-PRDX5 was purified as described previously [20].

2.3. Protection assay against oxidative single-strand breaks of plasmid DNA

pBR322 plasmid DNA (0.5 μg) was mixed with freshly prepared DTT (10 mM), $FeCl_3$ (3 μM) (MFO system) and recombinant human PRDX5 in a total volume of 20 μl of 50 mM HEPES (pH 7.0). Reaction mixtures (Chelex-100-eluted distilled water) were incubated for 90 min at 37 °C. Reactions were terminated by the addition of 4 μl of electrophoresis loading buffer. DNA samples were applied to 0.8% agarose gels in a TBE buffer and electrophoresis was performed at 100 mV for 1.5 h, at room temperature. After electrophoresis, the gel was stained with ethidium bromide, visualized under UV light and photographed. Quantitation was made by densitometric analyzes of the intensity of the bands using Kodak 1DV.3.5.3 software (Kodak Scientific Imaging Systems).

2.4. Cell culture

We used our previously established mito-PRDX5 CHO clone that stably overexpress human PRDX5 in mitochondria and the corresponding control cells (control CHO clone) which had been transfected with the expression vector without insert [13]. CHO-K1 cells were cultured in DMEM, 4.5 g D-glucose/l, supplemented with 10% fetal bovine serum, 100 U/ml penicillin, and 100 μg/ml streptomycin (complete DMEM) in a 95% humidified atmosphere, in 5% CO_2 at 37 °C. Overexpression of PRDX5 and mitochondrial localization in CHO cells was verified by immunofluorescence as previously described [11,13], using rabbit anti-human PRDX5 polyclonal antibody [22] and mouse monoclonal antibody directed to cytochrome C oxidase subunit 1 (COX1) (Molecular Probes).

2.5. Cell treatment with H_2O_2 and tBHP

1×10^6 CHO cells were seeded into 75 cm^2 culture flasks in complete DMEM. After 15–18 h of culture, 80% confluent cells were exposed to indicated concentrations of peroxide during one hour in DMEM without phenol red (4.5 g D-glucose/l) supplemented with 100 U/ml penicillin, 100 μg/ml streptomycin and 292 mg/l of L-glutamine (37 °C, 95% humidity, 5% CO_2). After treatment, cells were washed with PBS, harvested by trypsinisation and frozen at −80 °C until the isolation of total DNA.

2.6. Isolation of total DNA

High molecular weight DNA was isolated with the Dneasy Tissue Kit (Qiagen) as described by the manufacturer. The concentration of total cellular DNA was determined by DAPI fluorescence (exc. 370 nm and em. 460 nm). DNA samples were distributed into aliquots and frozen at −20 °C to avoid repeated freezing/thawing cycles.

2.7. Detection of oxidative mtDNA damages

Long PCR amplification of mtDNA was performed in a GeneAmp PCR system 2400 (Perkin–Elmer). Reaction mixtures contained 80 ng of total DNA, 2.75 mM $MgCl_2$, 500 μM deoxynucleotide triphosphates, 0.4 μM primers and 1.68 units of Expand Long Template polymerase (Roche) in a final volume of 20 μl. The primer nucleotide sequences were (see also Fig. 1): forward primer 5′-GGC TTA CAA GAT GCT ACG TCA CC-3′ (primer A), flanking the region of the cytochrome *c* oxidase subunit II gene (GenBank Accession No. AF455051) and reverse primer 5′-GGT AGG GTG GCT AGG ATT AGG ATG G-3′ (primer B), flanking the region of the cytochrome *b* gene (GenBank Accession No. AB033693). Prior to Expand Long Template polymerase addition, a hot start protocol was carried out that consisted of an initial cycle of 94 °C for 2 min and 80 °C for 2 min to ensure complete strand separation. The thermocycler profile included 30 cycles at 94 °C for 1 min, 64 °C for 1 min, 68 °C for 12 min, and final extension at 68 °C for 12 min. After long amplification, samples were diluted 100× and frozen at −20 °C until quantitation by real-time PCR. Quantitative real-time PCR was performed on the GeneAmp 7000 (ABI-PRISM), with the following primers (Fig. 1) hybridizing on NADH dehydrogenase subunit 4 gene (*ND4*; GenBank Accession No. NM_012094): forward primer 5′-CAC GAT AGC TAA GAT CCA AAC TGG G-3′ (primer C) and reverse primer 5′-GCC CAT TAC TTC CCA TCC CAT AGG C-3′ (primer D). The following TaqMan probe (Applied Biosystems), labelled with 5′-FAM and 3′-TAMRA was used: 5′-CGC TCA TGG TCT TAC ATC TTC TCT ACT ATT TTG TCT TGC-3′. PCR amplifications were carried out in TaqMan Universal PCR Master Mix (Applied Biosystems) with 0.2 ng DNA, 0.3 μM primers and 0.15 μM TaqMan probe in a final volume of 25 μl. To express the results in lesions per large PCR fragment, derived from the Poisson equation as described in Santos et al. [23], the threshold cycle values were plotted against the logarithm of DNA amounts for a series of known input templates and the DNA quantities of the unknown template were determined by linear regression.

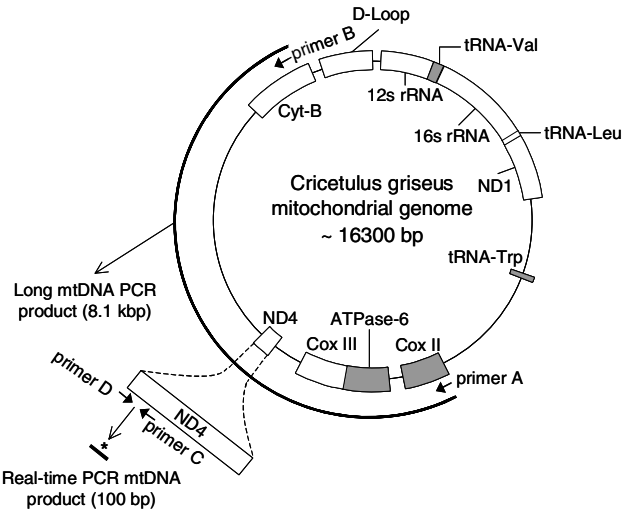

Fig. 1. Schematic representation of mitochondrial DNA of *Cricetulus griseus* and sequences amplified by PCR. The organization of the mitochondrial genome being very well conserved in rodents, the partially known *C. griseus* mitochondrial genome was represented according to the organization of the *Mus musculus* mitochondrial DNA. Partially sequenced coding sequences, tRNA and rRNA sequences are shown as white boxes. Complete coding sequences and tRNA sequences are shown as grey boxes. The 8.1 kbp long PCR amplification product is represented as a large arc. The 100 bp real-time PCR product is also represented. An asterisk indicates the TaqMan probe. The four primers used for PCR amplification are indicated by arrows (see also Section 2).

3. Results and discussion

3.1. Protective effects of PRDX5 against oxidative single-strand breaks of plasmid DNA

We investigated whether PRDX5 can directly protect DNA from single-strand breaks caused by metal catalyzed generation of ROS. In the MFO system, autoxidation of thiols (DTT) in the presence of iron generates ROS such as superox-

ide anion, H_2O_2 and hydroxyl radical (·OH) [24]. When generated very close to the nucleic acid molecule, hydroxyl radical can add hydrogen atoms to DNA bases or abstract hydrogen atoms from the sugar moiety, producing modified bases, DNA strand breaks or abasic sites [25]. Induction of single-strand breaks into supercoiled plasmid DNA (CCC DNA) leads to the formation of open circular plasmid DNA (OC DNA). Accordingly, DNA damages can be assessed by measuring the percentage of OC DNA on CCC DNA. As shown in Fig. 2A, incubation of plasmid DNA with the MFO system increased the formation of OC DNA. The addition of wt-PRDX5 resulted in an inhibition of the conversion of CCC to OC DNA in a dose-dependent manner. Wt-PRDX5 at 2 μM (36.6 μg/ml) or greater, completely protected plasmid DNA from the MFO system (Figs. 2A and D). Interestingly, TSA1, a yeast peroxiredoxin, was also tested for its DNA protective effects in similar conditions by Kwon and collaborators [19]. Complete DNA protection of TSA1 was observed from 3.7 μM (80 μg/ml), suggesting that wt-PRDX5 displays higher genoprotective properties.

Afterwards, we investigated whether recombinant nuc-PRDX5 can also directly protect DNA from damages induced by the MFO system (Figs. 2B and D). Indeed, this N-terminal-modified PRDX5, which allows a high expression of PRDX5 in the nucleus, was shown to protect nDNA against H_2O_2 and *t*BHP in CHO cells [13]. In the acellular assay, at 0.25 and 0.5 μM, nuc-PRDX5 inhibits the conversion of CCC to OC DNA similarly to wt-PRDX5 at the same concentrations (Figs. 2B and D). However, higher concentrations of nuc-PRDX5 produced migration anomalies. Indeed, at 1 μM, OC and CCC bands migrated slightly slower, while at 2–4 μM of nuc-PRDX5, plasmid DNA appeared as a high molecular weight smear (Fig. 2B). This modified DNA pattern concealed the genoprotective effects of nuc-PRDX5 at higher concentrations. The same DNA pattern of migration was observed in absence of the MFO system from 1 to 4 μM of nuc-PRDX5 (not shown). This modified migration pattern probably results from electrostatic interactions between the nuclear localization signal (NLS) lysine-rich amino acids and plasmid DNA, compacting the DNA and forming stable protein-DNA polyplexes when high protein concentrations of nuc-PRDX5 were used [26,27]. Finally, the genoprotective effects of wt- and nuc-PRDX5 were very similar at least at low protein concentrations. These results are reinforced by the fact that wt- and nuc-PRDX5 exhibited identical peroxidatic activities, in the presence of DTT or the thioredoxin system and in the presence of *t*BHP or H_2O_2 (not shown). All these results confirm that fusion of NLS at the amino-terminus of PRDX5 did not modify the catalytic properties of PRDX5. As a negative control, we used the catalytic mutant C47S-PRDX5, which is completely devoid of peroxidatic activities [16,21]. As shown in Figs 2C and D, this mutant exhibited a very limited DNA protection at the highest concentrations. This weak protection is probably due to unspecific quenching of ·OH by high concentrations of any proteins, as the latest are also cleaved with the MFO system [28].

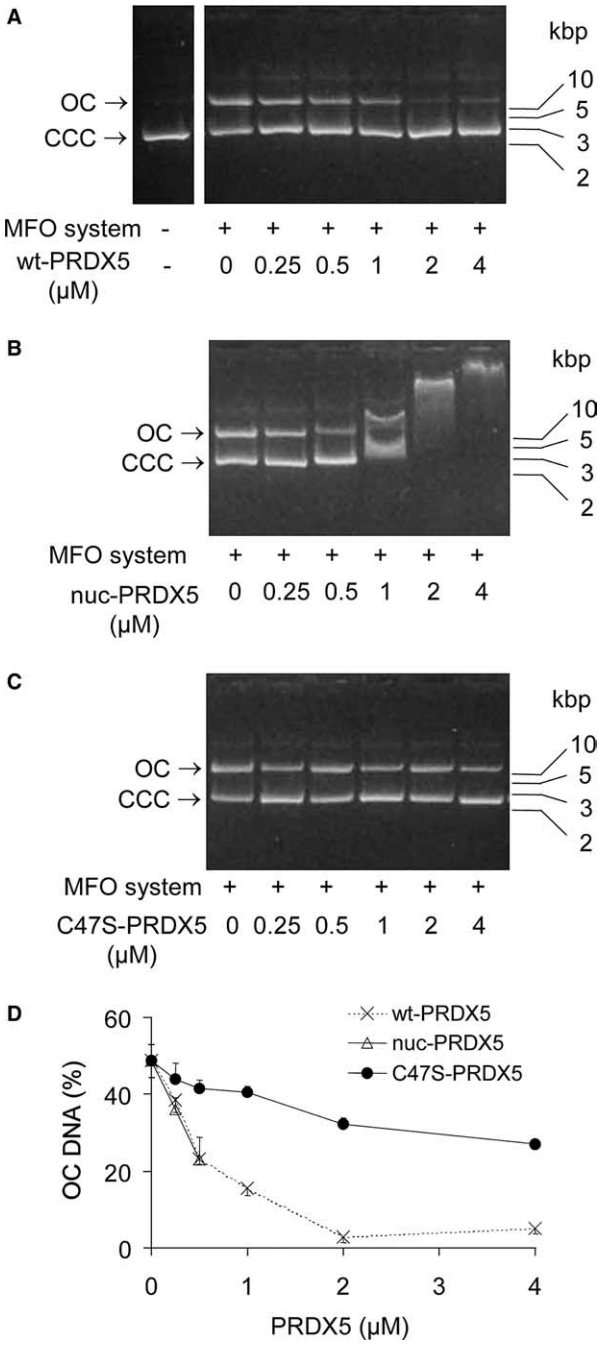

Fig. 2. Protective effects of different recombinant PRDX5 on DNA strand breaks induced by the MFO system. Protective effects of human wt-PRDX5 (A), nuc-PRDX5 (B), C47S-PRDX5 (C) at different concentrations. (D) Quantitation of the protection conferred by the different recombinant PRDX5 proteins against DNA strand breaks induced by the MFO system. Results are expressed as the percentage of plasmid open circular form (OC) on total plasmid DNA (OC + CCC). Values are means ± S.E.M. of results from five replicates in each case.

3.2. Genoprotective activities of PRDX5 on michondrial DNA

Long PCR amplifications of mtDNA were used to look for significant oxidative mtDNA damages in CHO cells. This method offers a broader measurement of the quality of the DNA, contrasting to more specific methods such as HPLC coupled with electrochemical detection [29]. Oxidative DNA damage, such as strand breaks, apurinic sites and some modified bases (for example, 8-OxodA) can hamper the progress of the polymerase [30,31]. So, a reduction in the relative yield of the long PCR product reflects the presence of blocking DNA lesions [23].

The frequency of mtDNA lesions was evaluated by a two-step PCR. First, long mtDNA fragments of 8.1 kbp were amplified by PCR using total DNA as template (Fig. 1). PCR amplification yield of such DNA fragments decreases with increasing amount of lesions [23]. Thus, in a second step, the yield of the long mtDNA PCR product was quantitated by real-time PCR, using primers and TaqMan probe hybridizing to *ND4*, localized in the middle of the long mtDNA PCR fragment (Fig. 1). Our long PCR conditions allowed the method to be quantitative. Indeed, a standard curve could be established between DNA quantities used as template in the long PCR and PCR amplicons detected by real-time PCR (Fig. 3). Results were normalized by quantitating each sample for the amount of initial mtDNA without previous long PCR amplification using the same real-time PCR conditions. As shown in Fig. 4, the decrease in the long PCR amplification, reflecting increased DNA lesions, appeared as a shift of the real-time PCR amplification curve to the right. By contrast, the real-time PCR amplification, without previous long PCR amplification, produced overlapping curves either with or without induced DNA damages, given that similar amounts of mtDNA quantities were used in the reaction.

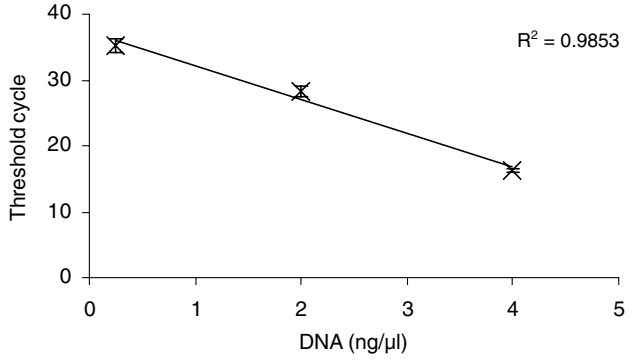

Fig. 3. Typical standard curve obtained by long PCR amplification of mtDNA and subsequent real-time PCR quantitation of *ND4* mtDNA with different concentrations of total DNA of CHO cells. In the long PCR amplification of mtDNA (see Fig. 1 and Section 2), different concentrations of total DNA from CHO cells (4, 2 and 0.25 ng/µl) were used. The products of long PCR amplifications were diluted 500-fold before performing real-time PCR quantitation of *ND4* mtDNA. This dilution was required due to the very high sensitivity of real-time PCR and to ensure a good linearity. Values are means ± S.E.M. of results from two replicates in each case.

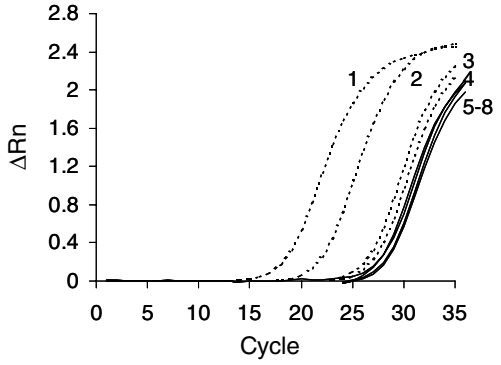

Fig. 4. Representative real-time PCR amplification curves of *ND4* mtDNA after exposure of control CHO cells to different concentrations of H_2O_2. Curves 1 and 5: 0 mM H_2O_2; curves 2 and 6: 0.2 mM H_2O_2; curves 3 and 7: 0.5 mM H_2O_2; curves 4 and 8: 1 mM H_2O_2. Curves 1–4 were obtained with previous long PCR amplification of 8.1 kbp mtDNA; curves 5–8 were obtained without previous long PCR amplification. Long and real-time PCR amplifications were performed as described in Section 2. ΔRn is the baseline substracted PCR product fluorescence normalized to an internal dye (ROX).

To determine whether mitochondrial PRDX5 can protect mtDNA against oxidative attacks, we submitted our previously established CHO clones overexpressing PRDX5 in mitochondria (mito-PRDX5 CHO) to exogenously applied H_2O_2 and *t*BHP for 1 h. Mito-PRDX5 CHO overexpressed human PRDX5 in mitochondria, up to 3.4 fold as previously quantitated by immunoblotting [13]. Co-localization of PRDX5 and cytochrome C oxidase (Fig. 5) showed that PRDX5 is constitutively localized to mitochondria in control CHO cells. Constitutive expression of PRDX5 in mitochondria has also been shown in other cell types, including HeLa cells, epithelial cells of rat kidney and bovine embryonic cells [16–18].

With increasing concentrations of H_2O_2 up to 1 mM, an increase of mtDNA damages was observed as measured by real-time PCR (Fig. 6A). Maximal mtDNA damages appeared at 0.5 mM and above, with ~6 lesions/8.1 kbp. At these concentrations, H_2O_2 prevented nearly totally the PCR amplification of mtDNA long fragments. Overexpressing PRDX5 in mitochondria of CHO cells significantly reduced mtDNA damages caused by exogenously added H_2O_2, completely at 0.2 mM and partially at 0.5 and 1 mM H_2O_2. H_2O_2 has been reported to damage mtDNA in many cell types. Indeed, Santos et al. [30] showed that a one hour exposure of human fibroblasts to H_2O_2 induced persistent mtDNA lesions even after long

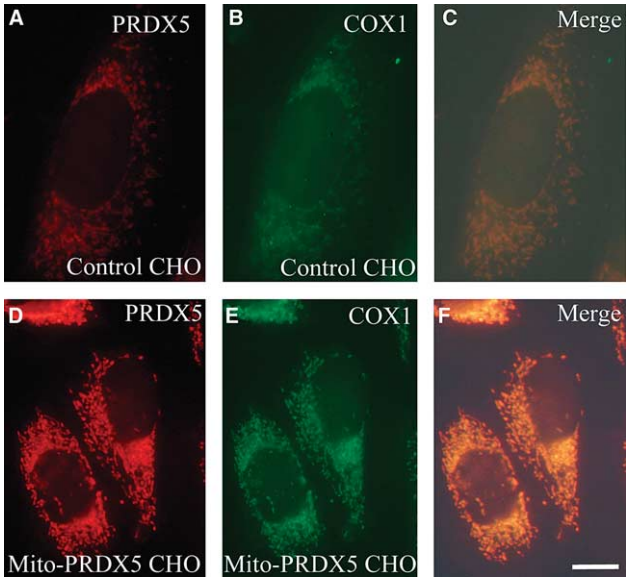

Fig. 5. Immunofluorescence analysis of subcellular localization of PRDX5 in CHO cells. Cultured control CHO cells transfected with pEF-BOS vector without insert (Control CHO; A, B, C) or cells transfected with pEF-BOS vector containing the cDNA sequence coding for PRDX5 with its mitochondrial presequence (Mito-PRDX5 CHO; D, E, F) were processed for immunofluorescence with antibodies directed to PRDX5 (A, D) and mitochondrial COX1 (B, E). Localization of PRDX5 in mitochondria either in control CHO or PRDX5 overexpressing cells was confirmed by co-localization of PRDX5 with COX1 as illustrated in merged images (Merge; C, F). Bar, 10 µM.

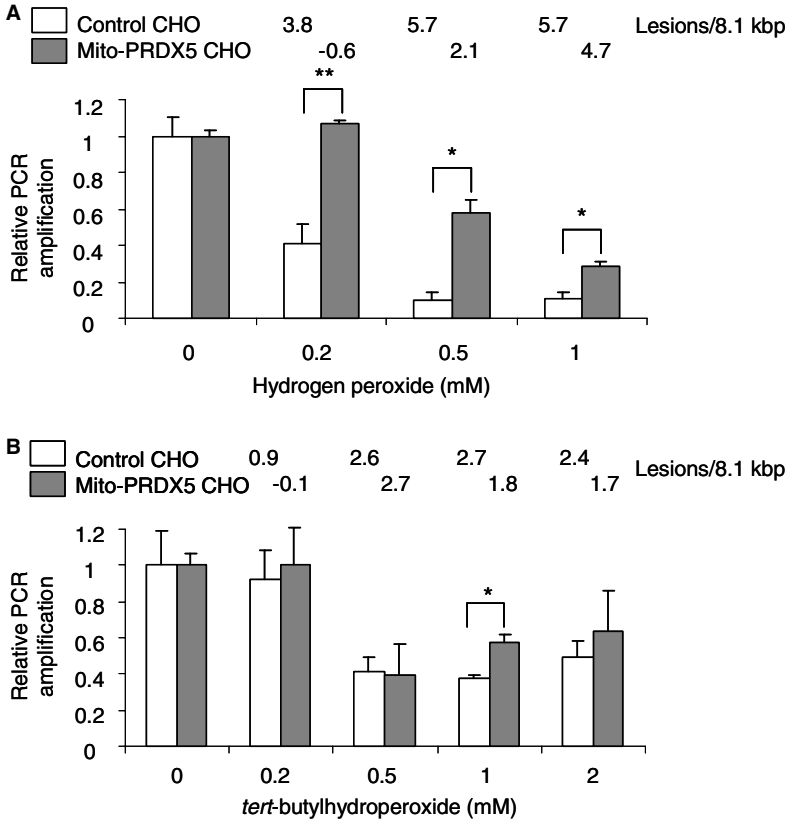

Fig. 6. MtDNA damages caused by H_2O_2 (A) and *t*BHP (B) in control CHO cells and in CHO cells overexpressing mitochondrial PRDX5 (mito-PRDX5 CHO). CHO cells were exposed to indicated concentrations of peroxides for 1 h. MtDNA damages were assessed by combined long PCR amplification and real-time PCR (see Section 2). Results are expressed as relative PCR amplification of mtDNA of peroxides-exposed CHO cells to corresponding unexposed controls. Results are also expressed in lesion frequency per large PCR fragment, derived from the Poisson equation as described in Santos et al. [23]. Values are means ± S.E.M. of results from four replicates in each case. Significance versus control is designated as $^{*}p < 0.05$ and $^{**}p < 0.001$ (Student *t* Test).

recovery periods. These damages are thought to be mediated by ·OH, resulting from Fenton reaction catalyzed by transition metals. Mitochondria are tightly involved in iron trafficking, due to synthesis of heme or Fe–S clusters [32]. Mitochondrial electron transport proteins contain iron–sulfur centers and are sensitive to ROS. Consequently, oxidative stress can liberate those protein iron contents that can lead to increased generation of ·OH within the inner mitochondrial matrix [33]. Mitochondrial PRDX5 could directly protect mtDNA, by reducing H_2O_2 and preventing the formation of ·OH close to mtDNA. PRDX5 could also indirectly protect mtDNA by maintaining the integrity of the mitochondrial electron transport chain, preventing the increased generation of ·OH within the inner mitochondrial matrix. MtDNA lesions have been suggested to be the initial event leading to a loss of mitochondrial membrane potential, cell growth arrest and subsequent cell death [30]. Besides, Yuan et al. [34] reported recently that cytosolic overexpression of PRDX5 could afford cell protection against apoptosis induced by H_2O_2 in human tendon cells.

MtDNA damages induced by *t*BHP, a short chain analog of lipid hydroperoxide, were also investigated in the present study. *t*BHP at concentrations of 0.5 mM or above increased mtDNA damages (Fig. 6B). However, these concentrations produced lower range of mtDNA damages (~2.7 lesions/8.1 kbp) than those observed for H_2O_2 (~5.7 lesions/8.1 kbp), suggesting that the propensity of *t*BHP to induce mtDNA damages is less important than for H_2O_2 in CHO cells. Restriction of the mitochondrial availability of suitable iron species for *t*BHP to produce mtDNA damages could explain the lowest level of mtDNA damages. Indeed, Byrnes et al. [35] reported that *t*BHP can react with a small subset of cell iron species which react with H_2O_2 to subsequently generate DNA strand breaks. To date, the nature of the iron species able to react with *t*BHP and to induce DNA damages is not fully characterized. As shown in Fig. 6B, overexpressing PRDX5 in mitochondria could afford more limited mtDNA protection against *t*BHP than against H_2O_2. However, in our previous study, mitochondrial overexpression of PRDX5 conferred the highest cell protection against *t*BHP [13]. As PRDX5 cannot afford high mtDNA protection against *t*BHP, increased cell survival probably resulted from PRDX5 protective effect on other cellular targets, such as membrane protein thiols. Indeed, *t*BHP can oxidize membrane protein thiols, leading to membrane disruption, NADPH depletion and finally loss of cell viability [36,37]. Finally, our current results strongly suggest that mtDNA is not a major target of *t*BHP in CHO cells. As a matter of fact, very few studies reported mtDNA damages induced by *t*BHP [38,39].

3.3. Conclusions and perspectives

Recently, compelling evidence implicated peroxiredoxins in genome maintenance [14]. Our previous studies showed genoprotective effects of PRDX5 on nDNA [13]. The present work

demonstrates the protective effects of mitochondrial PRDX5 on mtDNA in CHO cells. Considering its constitutive expression in mitochondria of many mammalian cell types [16–18, this study] as well as its genoprotective properties [13] and considering its highly conserved mitochondrial targeting throughout evolution [10,11,40], PRDX5 appears as a good candidate to protect mtDNA against oxidative damages caused by exogenous and endogenous ROS but also peroxynitrite [10]. Finally, it would be of interest to investigate whether expression levels of mitochondrial PRDX5 depending on the cell type could be linked to the vulnerability of mtDNA and whether this is relevant for somatic mitochondrial diseases.

Acknowledgements: This work was financially supported by the Fonds National de la Recherche Scientifique (FNRS) and by the Communauté française de Belgique-Actions de Recherche Concertées (ARC). Ingrid Banmeyer is recipient of a FRIA fellowship.

References

[1] Yakes, F.M. and Van Houten, B. (1997) Mitochondrial DNA damage is more extensive and persists longer than nuclear DNA damage in human cells following oxidative stress. Proc. Natl. Acad. Sci. USA 94, 514–519.
[2] Ljungman, M. and Hanawalt, P.C. (1992) Efficient protection against oxidative DNA damage in chromatin. Mol. Carcinog. 5, 264–269.
[3] Dizdaroglu, M., Rao, G., Halliwell, B. and Gajewski, E. (1991) Damage to the DNA bases in mammalian chromatin by hydrogen peroxide in the presence of ferric and cupric ions. Arch. Biochem. Biophys. 285, 317–324.
[4] Graziewicz, M.A., Day, B.J. and Copeland, W.C. (2002) The mitochondrial DNA polymerase as a target of oxidative damage. Nucleic Acids Res. 30, 2817–2824.
[5] Bohr, V.A. (2002) Repair of oxidative DNA damage in nuclear and mitochondrial DNA, and some changes with aging in mammalian cells. Free Radic. Biol. Med. 32, 804–812.
[6] Wallace, D.C. (1999) Mitochondrial diseases in man and mouse. Science 283, 1482–1488.
[7] Wood, Z.A., Schröder, E., Harris, J.R. and Poole, L.B. (2003) Structure, mechanism and regulation of peroxiredoxins. Trends Biochem. Sci. 28, 32–40.
[8] Chae, H.Z., Chung, S.J. and Rhee, S.G. (1994) Thioredoxin-dependent peroxide reductase from yeast. J. Biol. Chem. 269, 27670–27678.
[9] Bryk, R., Griffin, P. and Nathan, C. (2000) Peroxynitrite reductase activity of bacterial peroxiredoxins. Nature 407, 211–215.
[10] Dubuisson, M., Vander Stricht, D., Clippe, A., Etienne, F., Nauser, T., Kissner, R., Koppenol, W.H., Rees, J.F. and Knoops, B. (2004) Human peroxiredoxin 5 is a peroxynitrite reductase. FEBS Lett. 571, 161–165.
[11] Knoops, B., Clippe, A., Bogard, C., Arsalane, K., Wattiez, R., Hermans, C., Duconseille, E., Falmagne, P. and Bernard, A. (1999) Cloning and characterization of AOEB166, a novel mammalian antioxidant enzyme of the peroxiredoxin family. J. Biol. Chem. 274, 30451–30458.
[12] Watabe, S., Kohno, H., Kouyama, H., Hiroi, T., Yago, N. and Nakazawa, T. (1994) Purification and characterization of a substrate protein for mitochondrial ATP-dependent protease in bovine adrenal cortex. J. Biochem. (Tokyo) 115, 648–654.
[13] Banmeyer, I., Marchand, C., Verhaeghe, C., Vucic, B., Rees, J.F. and Knoops, B. (2004) Overexpression of human peroxiredoxin 5 in subcellular compartments of Chinese hamster ovary cells: effects on cytotoxicity and DNA damage caused by peroxides. Free Radic. Biol. Med. 36, 65–77.
[14] Wong, C.M., Siu, K.L. and Jin, D.Y. (2004) Peroxiredoxin-null yeast cells are hypersensitive to oxidative stress and are genomically unstable. J. Biol. Chem. 279, 23207–23213.
[15] Huang, M.E., Rio, A.G., Nicolas, A. and Kolodner, R.D. (2003) A genomewide screen in *Saccharomyces cerevisiae* for genes that suppress the accumulation of mutations. Proc. Natl. Acad. Sci. USA 100, 11529–11534.
[16] Seo, M.S., Kang, S.W., Kim, K., Baines, I.C., Lee, T.H. and Rhee, S.G. (2000) Identification of a new type of mammalian peroxiredoxin that forms an intramolecular disulfide as a reaction intermediate. J. Biol. Chem. 275, 20346–20354.
[17] Oberley, T.D., Verwiebe, E., Zhong, W., Kang, S.W. and Rhee, S.G. (2001) Localization of the thioredoxin system in normal rat kidney. Free Radic. Biol. Med. 30, 412–424.
[18] Leyens, G., Knoops, B. and Donnay, I. (2004) Expression of peroxiredoxins in bovine oocytes and embryos produced in vitro. Mol. Reprod. Dev. 69, 243–251.
[19] Kwon, S.J., Kim, K., Kim, I.H., Yoon, I.K. and Park, J.W. (1993) Strand breaks in DNA induced by a thiol/Fe(III)/O2 mixed-function oxidase system and its protection by a yeast antioxidant protein. Biochem. Biophys. Res. Commun. 192, 772–777.
[20] Declercq, J.P., Evrard, C., Clippe, A., Vander Stricht, D., Bernard, A. and Knoops, B. (2001) Crystal structure of human peroxiredoxin 5, a novel type of mammalian peroxiredoxin at 1.5 Å resolution. J. Mol. Biol. 311, 751–759.
[21] Plaisant, F., Clippe, A., Vander Stricht, D., Knoops, B. and Gressens, P. (2003) Recombinant peroxiredoxin 5 protects against excitotoxic brain lesions in newborn mice. Free Radic. Biol. Med. 34, 862–872.
[22] Wang, M.X., Wei, A., Yuan, J., Clippe, A., Bernard, A., Knoops, B. and Murrell, G.A. (2001) Antioxidant enzyme peroxiredoxin 5 is upregulated in degenerative human tendon. Biochem. Biophys. Res. Commun. 284, 667–673.
[23] Santos, J.H., Mandavilli, B.S. and Van Houten, B. (2002) Measuring oxidative mtDNA damage and repair using quantitative PCR. Methods Mol. Biol. 197, 159–176.
[24] Kim, K., Kim, I.H., Lee, K.Y., Rhee, S.G. and Stadtman, E.R. (1988) The isolation and purification of a specific protector protein which inhibits enzyme inactivation by a thiol/Fe(III)/O2 mixed-function oxidation system. J. Biol. Chem. 263, 4704–4711.
[25] Cooke, M.S., Evans, M.D., Dizdaroglu, M. and Lunec, J. (2003) Oxidative DNA damage: mechanisms, mutation, and disease. FASEB J. 17, 1195–1214.
[26] Ritter, W., Plank, C., Lausier, J., Rudolph, C., Zink, D., Reinhardt, D. and Rosenecker, J. (2003) A novel transfecting peptide comprising a tetrameric nuclear localization sequence. J. Mol. Med. 81, 708–717.
[27] Escriou, V., Carriere, M., Scherman, D. and Wils, P. (2003) NLS bioconjugates for targeting therapeutic genes to the nucleus. Adv. Drug Deliv. Rev. 55, 295–306.
[28] Kim, K., Rhee, S.G. and Stadtman, E.R. (1985) Nonenzymatic cleavage of proteins by reactive oxygen species generated by dithiothreitol and iron. J. Biol. Chem. 260, 15394–15397.
[29] Shigenaga, M.K., Gimeno, C.J. and Ames, B.N. (1989) Urinary 8-hydroxy-2′-deoxyguanosine as a biological marker of in vivo oxidative DNA damage. Proc. Natl. Acad. Sci. USA 86, 9697–9701.
[30] Santos, J.H., Hunakova, L., Chen, Y., Bortner, C. and Van Houten, B. (2003) Cell sorting experiments link persistent mitochondrial DNA damage with loss of mitochondrial membrane potential and apoptotic cell death. J. Biol. Chem. 278, 1728–1734.
[31] Sikorsky, J.A., Primerano, D.A., Fenger, T.W. and Denvir, J. (2004) Effect of DNA damage on PCR amplification efficiency with the relative threshold cycle method. Biochem. Biophys. Res. Commun. 323, 823–830.
[32] Arosio, P. and Levi, S. (2002) Ferritin, iron homeostasis, and oxidative damage. Free Radic. Biol. Med. 33, 457–463.
[33] Salazar, J.J. and Van Houten, B. (1997) Preferential mitochondrial DNA injury caused by glucose oxidase as a steady generator of hydrogen peroxide in human fibroblasts. Mutat. Res. 385, 139–149.
[34] Yuan, J., Murrell, G.A., Trickett, A., Landtmeters, M., Knoops, B. and Wang, M.X. (2004) Overexpression of antioxidant enzyme peroxiredoxin 5 protects human tendon cells against apoptosis and loss of cellular function during oxidative stress. Biochim. Biophys. Acta 1693, 37–45.

[35] Byrnes, R.W. (1996) Inhibition of hydroperoxide-induced DNA single-strand breakage by 1,10-phenanthroline in HL-60 cells: implications for iron speciation. Arch. Biochem. Biophys. 332, 70–78.
[36] Bryszewska, M., Piasecka, A., Zavodnik, L.B., Distel, L. and Schussler, H. (2003) Oxidative damage of Chinese hamster fibroblasts induced by t-butyl hydroperoxide and by X-rays. Biochim. Biophys. Acta 1621, 285–291.
[37] Mazhul, V., Shcherbin, D., Zavodnik, I., Rekawiecka, K. and Bryszewska, M. (1999) The effect of oxidative stress induced by t-butyl hydroperoxide on the structural dynamics of membrane proteins of Chinese hamster fibroblasts. Cell. Biol. Int. 23, 345–350.
[38] Mambo, E., Gao, X., Cohen, Y., Guo, Z., Talalay, P. and Sidransky, D. (2003) Electrophile and oxidant damage of mitochondrial DNA leading to rapid evolution of homoplasmic mutations. Proc. Natl. Acad. Sci. USA 100, 1838–1843.
[39] Suliman, H.B., Carraway, M.S., Velsor, L.W., Day, B.J., Ghio, A.J. and Piantadosi, C.A. (2002) Rapid mtDNA deletion by oxidants in rat liver mitochondria after hemin exposure. Free Radic. Biol. Med. 32, 246–256.
[40] Leyens, G., Donnay, I. and Knoops, B. (2003) Cloning of bovine peroxiredoxins-gene expression in bovine tissues and amino acid sequence comparison with rat, mouse and primate peroxiredoxins. Comp. Biochem. Physiol. B 136, 943–955.